ELSEVIER

Catalysis Today 36 (1997) 285–293

CATALYSIS TODAY

Conversion of syngas to light olefins over silicalite-1 supported iron and cobalt catalysts: Effect of manganese addition

Debasish Das *, Gopal Ravichandran, Dipak K. Chakrabarty

Solid State Laboratory, Chemistry Department, Indian Institute of Technology, Bombay 400 076, India

Abstract

An investigation of the syngas conversion to light olefins over manganese promoted iron and cobalt catalysts supported on silicalite-1 has been carried out. The addition of manganese to iron catalysts improves the olefin selectivity in syngas conversion. The XRD and Mössbauer results show that manganese reduces the particle size of iron oxide and thereby makes carburization difficult. Hägg carbide phase was found to be responsible for alkane formation and olefins are preferentially obtained in the presence of some oxides of Fe(+3). The addition of manganese to silicalite-1 supported cobalt catalyst was found to improve the CO conversion but the olefin selectivity was slightly decreased by the presence of manganese.

Keywords: Syngas conversion; Light olefins; Iron–manganese; Cobalt–manganese; Silicalite-1

1. Introduction

The production of liquid hydrocarbons from syngas via Fischer–Tropsch (FT) synthesis is a promising route for the production of clean fuels and chemicals from the vast sources of natural gas and coal. In the recent years there is an increasing demand for C_2–C_4 olefins which are the important raw materials for a number of chemical industries. At present the demand of these olefins are met by catalytic cracking of naphtha and dehydrogenation of alkanes. With the dwindling supply of petroleum feeds production of light olefins from coal derived syngas may become economically viable in the near future.

Conversion of syngas to gasoline range products has already been successfully commercialized (e.g., Salol plant in South Africa) and there is increasing interest in the design of a suitable catalyst for conversion of syngas to light olefins. The selective conversion of syngas to lower (C_2–C_4) olefins is an important commercial alternative to the production of liquid hydrocarbons. However, one of the most important limitation is the product selectivity. Although the chain growth mechanism of FT synthesis is governed by Anderson–Schulz–Flory kinetics, however, the limitations in product selectivity can be overcome by suitable selection of the catalyst and the process parameters. The chain growth process can be restricted after a few carbon atoms by containing the active metal particles (e.g., iron or cobalt) inside the small pores of a suitable support like zeolite [1–3].

* Corresponding author.

PII S0920-5861(96)00227-1

The activity and selectivity of such catalysts significantly vary depending on the nature of the zeolite support. It has been reported that the acidity of the zeolite support has a strong influence on the product pattern, e.g., medium pore acidic ZSM-5 zeolite supported iron catalysts yield a high fraction of aromatics [4–6] whereas, nonacidic silicalite-1 supported catalysts produce more olefins [7,8]. However, most of the catalyst formulations are iron-based and not much has been reported on cobalt-based catalysts. Synthesis of gasoline range hydrocarbons and aromatics has been reported on Co/ZSM-5 catalysts [6], whereas high selectivity for C_4 hydrocarbons has been observed on Co/NaY zeolite catalysts prepared from cobalt clusters [9]. Hydrocarbon products limited to a chain length of seven carbon atoms was also reported on Y and ZSM-5 zeolite supported cobalt catalysts [10].

It has been known for a long time that precipitated iron catalysts promoted with manganese shows stable activity and improved olefin selectivity [11–13], however, the role of manganese is not defined precisely. The aim of the present work is to investigate the effect of manganese addition to iron and cobalt catalysts supported on a neutral zeolite, silicalite-1.

2. Experimental

2.1. Catalyst preparation

Silicalite-1 was synthesized using the procedure given in the literature [14]. The zeolite was calcined in a flow of air at 550°C to decompose the organic template. Impregnation was carried out by adding the requisite amounts of 0.5 M iron or cobalt nitrate solution to freshly calcined support to achieve 10 wt.% metal loading. The manganese promoted catalysts were prepared by further addition of the requisite amount of 0.5 M manganese nitrate solution. In between two impregnations, the solid was dried at 100°C for 3 hours. The catalysts were designated as Sil–Fe(or Co)–Mn (x,y), where x and y represents the wt.% of iron (or cobalt) and manganese, respectively. The impregnated material was dried at 120°C for 12 hours and finally calcined at 450°C in air for 6 hours.

2.2. Catalyst characterization

Powder X-ray diffraction patterns of the zeolite support and the calcined samples were recorded in a Philips X-ray diffractometer PW 1820 with nickel filtered CuKα radiation. Transmission Mössbauer spectra of the calcined iron containing samples were recorded in a PC based multichannel analyzer using a 5 mCi ^{57}Co(Rh) source under constant acceleration mode. The instrument was calibrated with α-Fe absorber. The spectra were fitted using a computer program. Temperature programmed reduction (TPR) was studied in a home built apparatus. About 50 mg of the calcined sample loaded in a quartz tube was heated in argon flow at 400°C for 6 hours and then cooled down to room temperature in argon flow. The gas was then switched to 6% (v/v) hydrogen in argon (UHP, flow rate 55 ml/min) and the sample was heated at a rate of 10°C/min. The effluent gases were passed through a molecular sieve trap to remove traces of water formed during reduction and the amount of hydrogen consumed was detected by a thermal conductivity detector.

2.3. Syngas conversion

The catalytic performances in syngas conversion was evaluated in a high pressure continuous flow fixed bed microreactor (BTRS-Jr, Autoclave Engineers, USA) having online analytical provisions. 1 g of the calcined catalyst (particle size 180–300 mesh) was packed in the reactor between quartz wool plugs and reduced in-situ in a flow of hydrogen (20 ml/min) at 450°C for 12 hours prior to reaction. The feed

gas (premixed CO and H_2) was used without further purification. Reactants and products were analyzed by gas chromatography. Hydrocarbon products were separated on a 6 ft × 1/8 in. Porapak Q column and then analyzed by flame ionisation detector. The column detects upto C_7 hydrocarbons and clearly separates olefinic and paraffinic components upto 4 carbon atoms. Carbon monoxide, carbon dioxide, hydrogen and argon (internal standard) were separated by using a 6 ft × 1/4 in. CTR-1 column and analyzed in a thermal conductivity detector. The detailed reaction setup and analytical procedures were described earlier [15].

3. Results and discussion

3.1. Iron–manganese catalysts

X-ray diffraction patterns of the calcined Fe/Sil sample showed two weak lines at $d =$ 2.71 and 2.50 Å due to the presence of α-Fe_2O_3. However, the manganese promoted iron samples showed only the XRD lines for the zeolite support. This shows that the addition of manganese reduces the particle size of iron oxide making them X-ray amorphous.

Mössbauer spectra of the calcined Fe/Sil and Fe–Mn/Sil catalysts containing varying amount

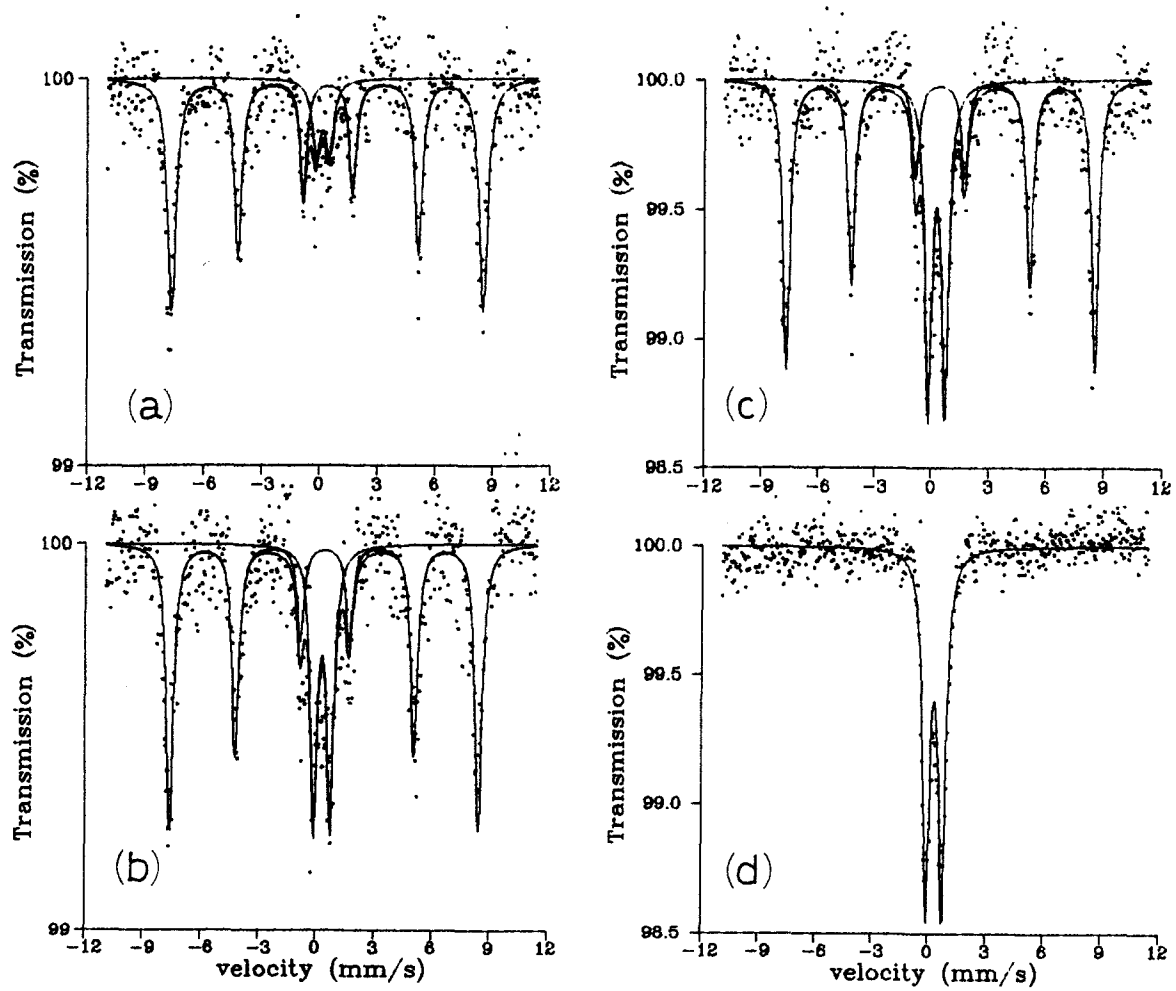

Fig. 1. Mössbauer spectra of calcined samples (a) Sil–Fe–Mn (10,0); (b) Sil– Fe–Mn (10,5); (c) Sil–Fe–Mn (10,10); (d) Sil–Fe–Mn (10,20).

Table 1
Mössbauer parameters of the calcined iron–manganese catalysts

Sample	Species	I.S. (mm/s)	Q.S. (mm/s)	H.F Field (kG)	Area (%)
Sil–Fe–Mn (10,0)	α-Fe_2O_3	0.44	0	503	87
	SPO	0.15	0.68		13
Sil–Fe–Mn (10,5)	α-Fe_2O_3	0.39	0	498	68
	SPO	0.28	0.85		32
Sil–Fe–Mn (10,10)	α-Fe_2O_3	0.44	0	503	64
	SPO	0.28	0.87		36
Sil–Fe–Mn (10,20)	α-Fe_2O_3				
	SPO	0.31	0.83		100

of manganese are shown in Fig. 1. The spectra consists of a sextet due to α-Fe_2O_3 and a central doublet due to small particles of superparamagnetic iron oxide (SPO). Calculation of the area ratio of the sextet and doublet shows that with the addition of manganese the amount of superparamagnetic oxide phase increases in the samples (Table 1). These findings along with the X-ray results prove that manganese increases the dispersion of iron oxide phase by reducing their particle size.

The results of syngas conversion over unpromoted and manganese promoted iron catalysts are presented in Table 2. It was observed that in comparison to the earlier work reported by Rao et al. [7] the unpromoted iron catalyst of the present work showed very good olefin selectivity under almost identical operating conditions. Addition of manganese as a promoter was found to further improve the olefin selectivity. Thus, the O/P ratio continuously increased from 8.4 (for unpromoted iron catalysts) to 13.1 (for Sil–Fe–Mn (10,20). However, this increase was not very appreciable beyond 10 wt.% manganese addition.

Fig. 2 shows the variation of olefin/paraffin ratio for products with different carbon numbers. It can be seen that a dramatic increase in O/P ratio of C_3 products was obtained at 5 wt.% manganese addition. For C_2, the O/P

Table 2
Syngas conversion over silicalite-1 supported iron and iron–manganese catalysts Temperature = 275°C, Pressure = 21 atm, GHSV = 1200 h^{-1}, $H_2/CO = 1$

Catalyst	Sil–Fe	Sil–Fe [a]	Sil–Fe–Mn	Sil–Fe–Mn	Sil–Fe–Mn	ZSM-5–Fe–Mn
Fe Loading (wt.%)	10	13.6	10	10	10	10
Mn Loading (wt.%)	0	0	5	10	20	10
CO conversion (mol %)	7.1	na	5.2	10.4	16.4	13.2
CO conv to CO_2 (mol %)	1.2	na	0.7	2.7	3.5	1.8
Product distribution (wt.%)						
C_1	11.2	18.6	9.3	9.3	8.6	27.4
$C_2^=$	11.1	3.8	17.4	13.0	12.7	1.5
C_2	2.7	11.5	2.6	2.3	2.0	13.4
$C_3^=$	19.6	11.1	29.3	23.6	23.3	1.4
C_3	1.1	5.5	0.6	0.9	0.9	12.9
$C_4^=$	13.9	0.0	18.6	17.0	17.9	1.4
C_4	1.5	0.0	2.9	1.1	1.2	18.1
C_{5+}	39.0	41.8	19.4	32.7	33.5	23.9
O/P	8.4	0.9	10.7	12.5	13.1	0.1

(a) GHSV = 1000 h^{-1}, Temperature = 280°C ref. [7].
na = not available.

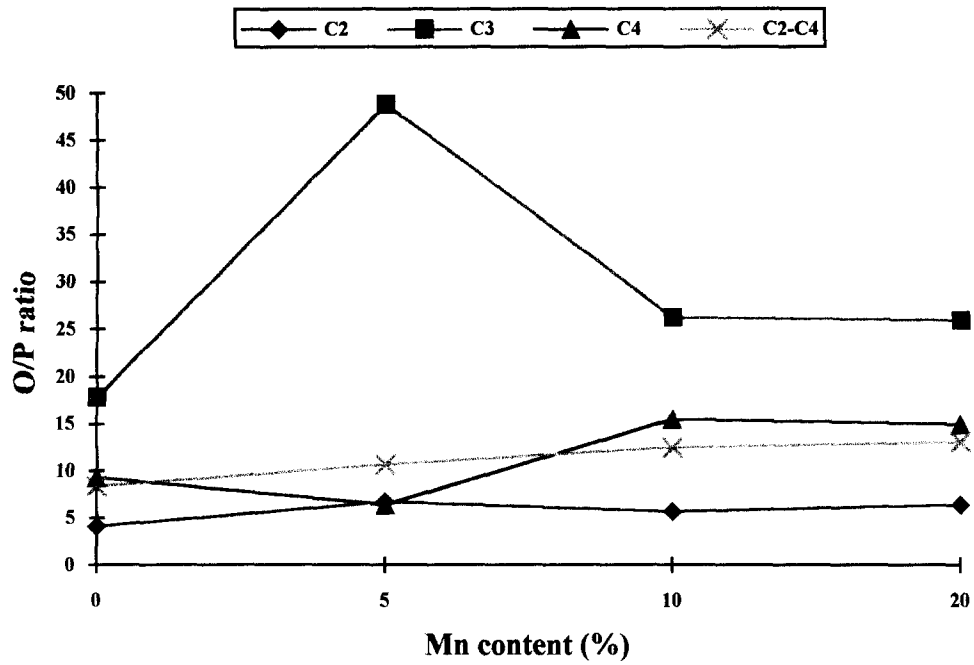

Fig. 2. Variation of O/P ratios of C_2, C_3, C_4 and C_2–C_4 products with Mn content.

ratio did not change much with manganese addition, while for C_3 it reached the maximum with about 5 wt.% manganese. Fig. 2 also shows that the O/P ratio remained almost constant beyond 10 wt.% manganese addition.

It is interesting to note that Sil–Fe–Mn (10,10) and Sil–Fe–Mn(10,20) which have very different Mössbauer patterns have very similar O/P selectivity and product patterns. This is due to the reason that the *active* catalyst which is formed during reduction and initial period of reaction is very different from the calcined samples. The olefin selectivity of the catalysts will depend on the relative amount of the different phases present in the *active* catalyst. It may be possible that the relative amount of the active phase(s) responsible for olefin formation are same in these two catalysts resulting in similar olefin selectivity and product pattern.

It is well known that during the reductive atmosphere of syngas reaction iron catalysts undergo rapid changes and convert mostly to metallic iron or iron carbides.

$$Fe_2O_3 \rightarrow Fe_3O_4 \rightarrow Fe_5C_2.$$

Although it has been noticed that the activity of iron catalysts parallels to the amount of carbide formation [16–19], it is still not clear whether iron carbide or iron oxide phase is responsible for olefin formation. Raymond et al. [20,21] observed very high syngas conversion activity in the presence of Fe_3O_4 but they did not report the olefin selectivity of their catalysts. Recently, Itoh et al. [22] reported Fe_2C phase to be the most favourable species for olefin formation at CO conversion level below 40% and found that at higher CO conversion level the Fe_3O_4 and $Mn_xFe_{3-x}O_4$ phases are responsible for olefin selectivity. They concluded that the formation of mixed oxide enhances the olefin selectivity of the iron–manganese catalysts. In the present work, we did not observe any formation of the Fe_2C phase. Mössbauer spectra of the used catalysts rather indicated the formation of Hägg carbide and presence of some Fe(+3) oxide phase. Table 3 shows the relative amount of the Hägg carbide in the used catalysts and it can be seen that the addition of manganese inhibits the formation of Hägg carbide phase. This is due to

Table 3
Relative area ratios of Hägg carbide and oxide phase in the used iron–manganese catalysts

Catalyst	Hägg carbide	Fe (+3) oxide phase
Sil–Fe–Mn (10,0)	85	15
Sil–Fe–Mn (10,5)	80	20
Sil–Fe–Mn (10,10)	79	21
Sil–Fe–Mn (10,20)	71	29

the reason that the addition of manganese reduces the particle size of iron oxide and thereby makes it relatively difficult to carburize them.

While manganese addition decreased the relative amount of Hägg carbide phase in the catalysts, on the other hand, it enhanced the O/P selectivity continuously. These observations clearly indicate that the presence of Hägg carbide phase is not responsible for olefin formation rather it may be related to the presence of Fe_3O_4 or $Mn_xFe_{3-x}O_4$ phase in the unpromoted and manganese promoted iron catalysts, respectively.

In Fig. 3 the olefin selectivity of the catalysts are plotted against time on stream. It shows that for manganese free iron catalyst the O/P selectivity reached a steady value within one hour of reaction time, whereas for the manganese promoted catalysts it increased continuously upto 3 hour and after that did not change much. Most possibly the phase responsible for olefin formation forms more readily in iron catalysts and slowly in manganese promoted catalysts.

Table 2 also shows that acidity of the support has a strong influence on the final product pattern. Thus, ZSM-5–Fe–Mn and Sil–Fe–Mn (10,10) catalysts with similar iron and manganese content has very different olefin selectivity. This is not unusual because ZSM-5 and silicalite (both having identical crystal and pore structure) have very different acidity. The former has strong acid sites which favour secondary reactions of alkenes whereas silicalite is nonacidic in nature. As a consequence the O/P ratio was much lower on ZSM-5 supported catalysts.

Carbon dioxide is formed during syngas conversion reaction by the secondary Water–gas shift (WGS) reaction. As it results in the forma-

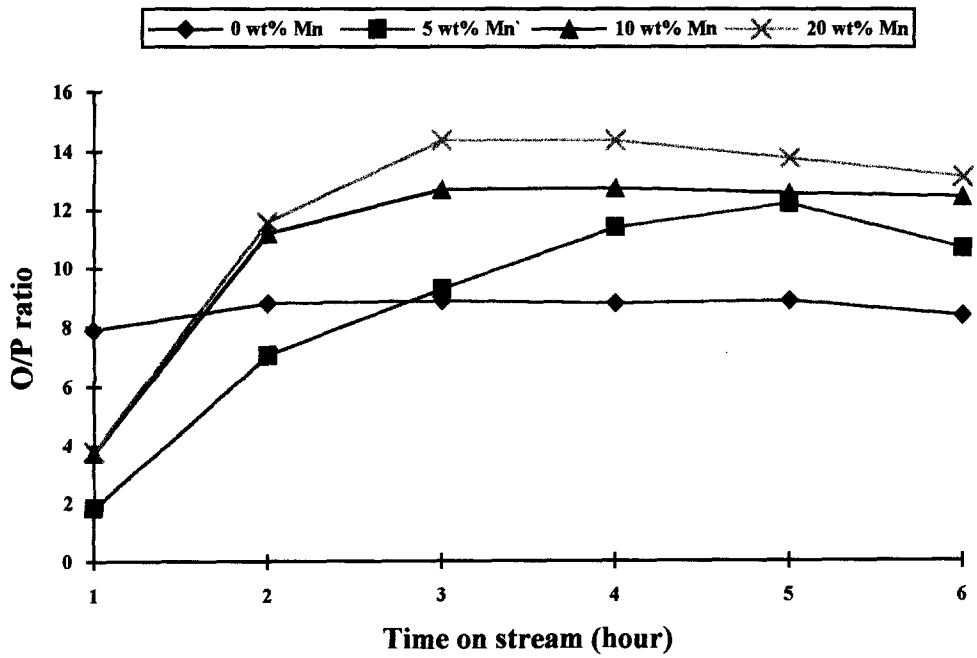

Fig. 3. Variation of O/P ratios with TOS for catalysts with different Mn content.

tion of undesired byproduct it is important that a good FT catalyst should have low water–gas shift activity. It is well known that Fe_3O_4, which forms in the reductive atmosphere of syngas conversion, promotes WGS activity. Fig. 4 shows the variation of CO conversion, selectivity to CO_2 and the HC/CO_2 with manganese content of the catalysts. It can be seen that the HC/CO_2 ratio was maximum at 5 wt.% manganese addition and further addition of manganese has a negative effect on this.

3.2. Cobalt–manganese catalysts

The XRD pattern of calcined Sil–Co sample showed two lines at $d = 2.84$ and 2.43 Å indicating presence of Co_3O_4 phase. With the addition of manganese these two lines disappeared but unlike iron catalysts the manganese promoted cobalt catalyst showed a new peak at $d = 2.47$ Å which is due to the mixed spinel M_3O_4 (where M is either Mn or Co). Calcination of the sample at higher temperatures showed an increase in intensity of this line indicating more abundance of this phase.

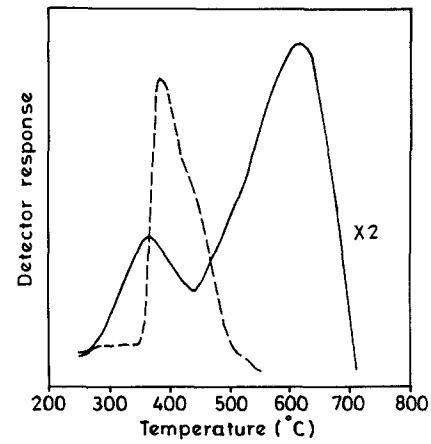

Fig. 5. Temperature programmed desorption patterns of Sil–Co (- - -) and Sil–Co–Mn (————) samples.

The temperature programmed reduction behaviour of the catalysts is shown in Fig. 5. While manganese free cobalt sample was reduced in a single step with the peak maximum at 390°C, the manganese promoted catalyst was reduced in two distinct steps. The low temperature peak at 370°C may be assigned to the reduction of Co_3O_4 phase. The other high temperature peak was due to the reduction of the

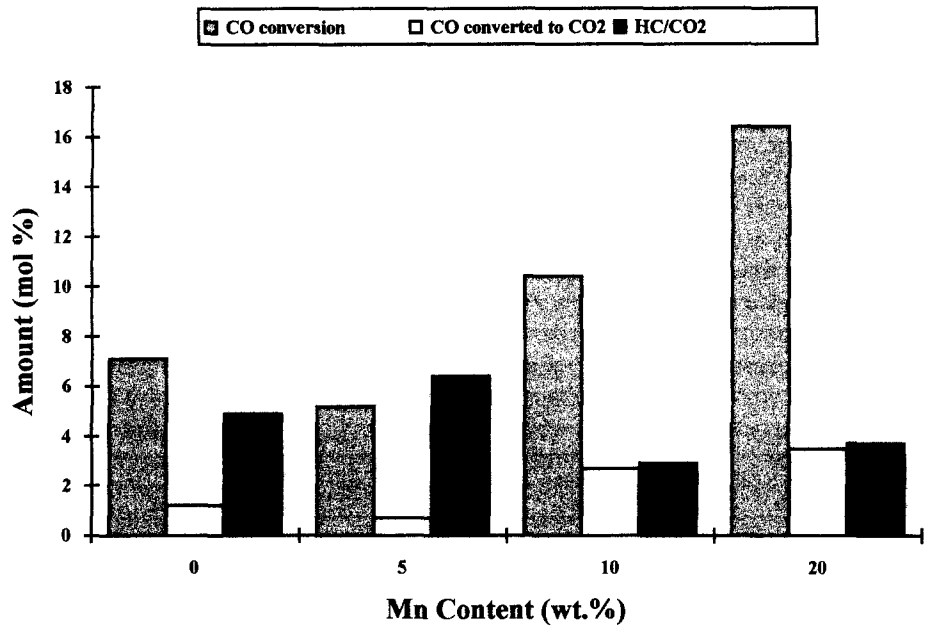

Fig. 4. Variation of CO conversion, selectivity to CO_2 and HC/CO_2 ratio with Mn content.

Table 4
Syngas conversion over silicalite-1 supported cobalt and cobalt–manganese catalysts

Catalyst	Sil–Co	ZSM-5–Co [a]	Sil–Co [b]	Co(ppt) [c]	Sil–Co–Mn	Co–Mn (ppt) [c]
Co Loading (wt.%)	10	9	4	100	10	50
Mn loading (wt.%)	0	0	0	0	10	50
Pressure	21	21	1	7	21	6
H_2/CO	3	1	2	1	3	1
Temperature (°C)	250	280	250	220	250	220
Sp. velocity (h^{-1})	1200	na	1200	279	1200	250
CO conversion (mol %)	20.2	56.5	5.7	43.9	33.9	42.9
CO conv to CO_2 (mol %)	3.4	na	0.9	na	6.2	na
Product distribution (wt.%)						
C_1	17.4	24.4	19.0	19.0	19.6	8.5
$C_2^=$	7.9	0.0	4.0	0.2	6.5	3.3
C_2	3.7	2.7	4.0	3.4	3.6	3.6
$C_3^=$	12.0	0.8	12.5	2.1	13.2	16.1
C_3	3.7	2.7	1.5	3.9	4.6	3.7
$C_4^=$	8.8	0.8	11.0	–	10.2	–
C_4	2.2	5.4	2.0	5.7 *	5.2	10.0 *
C_{5+}	44.4	63.0	65.0	63.6	37.0	46.9
O/P	3.0	0.1	3.6	0.3	2.3	2.7

[a] Ref. [6]; [b] Ref. [23]; [c] Ref. [24]; (na) not available; * Total C_4.

$(Co_{1-x}Mn_x)_3O_4$ phase as confirmed by using pure mixed oxide phase under identical conditions.

The results of syngas conversion over cobalt and cobalt–manganese catalysts are given in Table 4. The results obtained in this work has been compared with other catalysts reported in the literature. As expected the support acidity has a strong influence on the product pattern. ZSM-5 which has identical crystal and pore structure as silicalite-1 yields very low O/P ratio and mostly gave higher hydrocarbon fractions. With almost identical cobalt loading the silicalite-1 supported catalyst showed much higher olefin selectivity even at H_2:CO ratio of 3. Comparison with the earlier work of Peukert et al. [23] showed that the catalyst studied in the present work showed almost similar O/P ratio. The higher conversion of the present catalyst system was possibly due to the higher metal loading. Olefin selectivity of the Sil–Co catalyst was found to be much higher than that of precipitated catalysts. The low olefin selectivity of precipitated catalysts was possibly due to high hydrogenation activity of this catalyst [24]. Another explanation may be that at low space velocity and high CO conversion level the primary products formed may undergo further secondary reactions resulting in a low O/P value.

Addition of manganese to silicalite-1 supported cobalt catalyst increased the CO conversion but it also increased the amount of CO_2 in the product. However, unlike iron catalysts the olefin selectivity was not affected by the addition of manganese. It was found that on the basis of cobalt content of the catalysts the silicalite supported catalyst has better activity than precipitated catalyst.

4. Conclusions

Iron and cobalt catalysts supported on silicalite-1 showed good activity and selectivity for light olefins synthesis from syngas. Addition of manganese to iron catalysts reduces the iron oxide particle size and thereby makes carburization difficult. Increased olefin selectivity is related to the presence of Fe(+3) phase in the active catalyst. High selectivity for C_3 olefin was obtained with catalyst having 10 wt.% iron and 5 wt.% manganese.

In calcined Sil–Co catalyst, Co_3O_4 was found to be only phase present, while manganese-promoted cobalt catalyst showed presence of the mixed oxide phase. Addition of manganese facilitates the reduction of Co_3O_4 phase and also possibly reduces its particle size. Although manganese addition to cobalt catalyst increased CO conversion, however, it did not improve the olefin selectivity.

Acknowledgements

This work was supported by a research grant from the Department of Science and Technology, New Delhi.

References

[1] S. Kawi, J.R. Chang and B.C. Gates, J. Am. Chem. Soc., 115 (1993) 4830
[2] P.L. Zhou, S.D. Malone and B.C. Gates, J. Catal., 129 (1991) 315.
[3] H.H. Nijs, P.A. Jacobs and J.B. Uytterhoeven, J. Chem. Soc. Chem. Commun., (1979) 180.
[4] C.D. Chang, W.H. Lang and A.J. Silvestri, J. Catal., 56 (1979) 268.
[5] J.A. Caeser, J.A. Brennan, W.E. Garwood and J. Ciric, J. Catal., 56 (1979) 274.
[6] V.U.S. Rao, R.J. Gormley, R.R. Schehl, K.H. Rhee, R.D.H. Chi and D. Pantages, in: R.G. Herman, Ed., Catalytic Conversion of Synthesis Gas and Alcohols to Chemicals, Plenum, NY, 1984, p. 151.
[7] V.U.S. Rao and R.J. Gormley, Hydro. Proc., 59 (1980) 139.
[8] V.U.S. Rao, R.J. Gormley, L.C. Schneider and R. Obermyer, Am. Chem. Soc. Div. Fuel Chem. Prepr., (1980) 119.
[9] L.F. Nazar, G. Ozin, F. Hugues, J. Godber and D. Rancourt, Angew. Chem. Intl. Ed. Engl., 22 (1983) 624.
[10] G. Fornasari, T.M.G. La Torretta, A. Vaccari, S. Bednarova, P. Jiru and Z. Tvaruzkova, Stud. Surf. Sci. Catal., 61 (1993) 333.
[11] B. Büssemeier, C.D. Frohning and B. Cornlis, Hydro. Proc., 55 (1976) 105.
[12] H. Kölbel, M. Ralek and K.O. Tillmetz, in: Proc. 13th Intersoc. Energy Conv. Eng. Conf., Society of Automotive Eng., San Diego, 1978, p. 482.
[13] J. Barrault, C. Forquy and V. Perrichon, Appl Catal., 5 (1983) 119.
[14] C.V.V. Satynarayana and D.K. Chakrabarty, Appl. Catal., 66 (1990) 1.
[15] D. Das, G. Ravichandran, D.K. Chakrabarty, S.N. Piramanayagam and S.N. Shringi, Appl. Catal., 107 (1993) 73.
[16] G.B. Raupp and W.N. Delgass, J. Catal., 58 (1979) 348, 361.
[17] H.P. Bonzel and H.J. Krebs, Surf. Sci., 91 (1980) 499.
[18] D.J. Dwyer and H.J. Hardenbergh, J. Catal., 87 (1984) 66.
[19] H.J. Krebs, H.P. Bonzel, W. Sebwarting and G. Gafaer, J. Catal., 63 (1980) 226.
[20] J.P. Reymond, P. Mériandeau and S.J. Teichner, J. Catal., 75 (1982) 39.
[21] F. Blanchard, J.P. Reymond, B. Pommier and S.J. Teichner, J. Mol. Catal., 17 (1982) 171.
[22] H. Itoh, S. Nagano, K. Takeda and E. Kikuchi, Appl. Catal., 96 (1993) 125.
[23] M. Peukert and G. Linden, in: Proc. 8th Int. Congr. Catalysis, Berlin, Verlag Chemie, Weinheim, Vol. 2, 1984, p. 135.
[24] M. van der Riet, R.G. Copperwhaite and G.J. Huchings, J. Chem. Soc. Farad. Trans., 83 (1980) 2963.